

Self-Controlled Switchable Current Sharing Path for Multi-Receiver Wireless Power Transfer Systems

Ahmet Halis Sabırlı, Enes Ayaz, Ozan Keysan

Abstract—This paper presents a self-controlled current balancing method via a switchable current sharing path for multi-receiver (multi-Rx) wireless power transfer (WPT) systems. Conventional methods utilize a continuous current-sharing path, but it has drawbacks, such as higher circulation current and lower efficiency in strong misalignment or fault cases. Therefore, using modular structures to achieve misalignment-tolerant and high-efficient systems in high-power applications becomes challenging. In the proposed system, the current sharing path turns on within a specified misalignment ratio and turns off in fault or strong misalignment conditions. Also, the proposed system drives the switches using directly induced receiver voltages which are monitored with only passive elements, so the requirements of an Rx-side controller and gate drives for the switches are eliminated. An experimental setup of the 1Tx-2Rx system is established and tested for different misalignments and fault cases. In the proposed system, it is observed that 400 W power is transferred with efficiencies between 80% and 90% under different conditions. Accordingly, it is concluded that the efficiency and misalignment-tolerance increase compared to conventional systems.

Index Terms—Wireless power transfer, multi-receiver, current balancing, modular structure

I. INTRODUCTION

Inductive power transfer (IPT) systems are becoming increasingly popular in industrial applications since they offer several benefits over traditional wired power systems [1], [2]. They improve safety, portability, reliability, and efficiency thanks to eliminating the need for electrical cables and the need to be tethered to a power source [3]–[5]. Although IPT systems fit low-power consumer electronic products, the industry faces applying them in high-power applications to benefit from its advantages [6]. However, some challenges in high-power applications, such as transfer efficiency and misalignment tolerance, reveal. In order to improve them, modular structure in IPT systems, where a circuit diagram is given in Fig. 1, comes to the forefront [7], [8].

The modular structure allows the system to be easily customized and scaled to meet the application's specific ratings [9]. Besides, the connection of modules (parallel or series structures) allows utilizing the semiconductors with lower current or voltage ratings, which enables using standardized components [10]. Moreover, modular structure simplifies thermal management and increases efficiency by sharing power and losses. Furthermore, they can be designed with built-in redundancy [6]. If one module fails, the system can continue its operation using the remaining modules, which increases

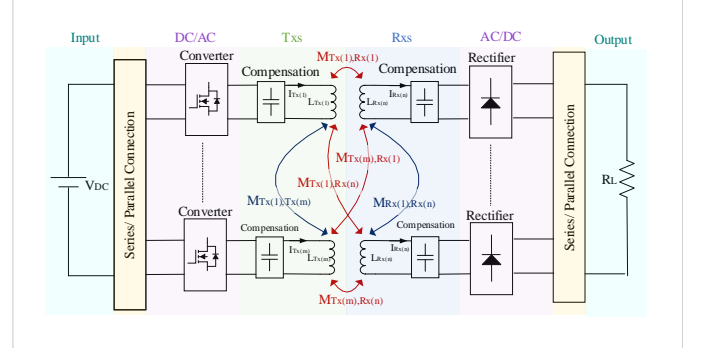


Fig. 1. The circuit diagram of a modular inductive power transfer system.

reliability. However, modularity comes with its own challenges, and it is observed that they are susceptible to slight misalignment, which can be stemmed from movement (due to the nature of dynamic applications), and manufacturing tolerances [11]–[13]. That is to say, modular systems have power-sharing issues between the modules (Tx or Rx) due to parameter variation, especially mutual inductance variation. The one drawback of the unbalanced power distribution is to exceed the voltage/current ratings of the modules if the modules are not over-designed. Another drawback is to decrease the efficiency because if the power flows dominantly along fewer modules, and so ohmic losses increase. Further, due to these drawbacks, unequal power distribution causes early aging modules and reliability problems. Therefore, in a modular system, the unequal power distribution issue due to misalignment stemming from the nature of dynamic applications or manufacturing tolerances should be solved.

The unequal power distribution issue may occur in Tx modules or Rx modules. At first, for multi-Tx structures, it can be solved by just applying a control algorithm since Tx modules have active DC/AC converters. In [14], a d-q frame control is given in order to balance the current for parallel Tx and minimize the circulating current. In [15], multiphase Tx modules are proposed by employing a hybrid phase frequency control strategy. However, in order to avoid control complexity, passive methods are also introduced. In [16], introducing coupled inductors with a cyclic cascade connection is proposed. In [17], [18], a path is introduced to achieve passive and automatic current sharing. In [19], passive-impedance-matching by parallel connected additional inductance is introduced to achieve automatic current sharing for multi-Tx. Afterward, for multi-Rx structures, the solution for Tx modules can also be applied, but it is recalled that

Ahmet Halis Sabırlı, Enes Ayaz, and Ozan Keysan are with the Department of Electrical and Electronics Engineering, Middle East Technical University, Ankara, Turkey

Corresponding Author: Ozan Keysan, keysan@metu.edu.tr

Rx modules usually are made up of passive rectifiers. Therefore, just only applying control algorithms is not possible without the addition of hardware, such as post-regulation converters, which increases the control complexity and cost. Hence, passive balancing methods gain more importance for Rx modules. In [20], it is proposed that detuning the receive side is a viable option to reduce unbalanced in addition to cross-coupling between the Rx modules. In [21], to solve this power-sharing issue, a middle-stage resonator is introduced, and in this system, balanced power transfer still continues even in the case of a fault. In [22], the current sharing path is introduced, like applied on Tx-side. However, in the case of fault and strong misalignment, it is observed that these passive balancing methods create a circulating current and disturb the fault tolerance.

In this paper, a new current balancing method for multi-Rx systems that is powered and controlled by the induced voltages of Rx coils without an additional controller and gate drives is introduced to create a switchable current-sharing path between receivers. The proposed system avoids unbalanced power transfer between the receivers, and also, in the case of fault or strong misalignment, it disconnects the current sharing path by tracking the receiver coil voltages with self-control.

The remaining parts of the paper are as follows. Section II gives the system structure of a multi-receiver system. Section III defines the current sharing problem with a mathematical model. Section IV analyses the conventional current sharing path methods for misalignment and fault conditions. Section V introduces the proposed method. Section VI gives experimental validation.

II. SYSTEM STRUCTURE

The proposed system aims for a modular structure for WPT systems to achieve a misalignment-tolerant and increase efficiency. While misalignment occurs, the coupling coefficient between Tx-Rx modules may change drastically. On the one hand, the changes can reduce the transferred power, and a modular structure was already introduced to avoid it. On the other hand, the system's resonance frequency may also vary due to the change in the coupling coefficients. Since series-series compensation topology gives load and coupling independent resonance frequency, in the proposed system, series-series topology is considered more suitable than other topologies. However, series-series topology has a drawback in the cases of no-load and zero coupling. The system draws a short circuit current in such cases. The couplings between Tx and Rx may reduce to almost zero due to misalignment, which causes a short circuit current. Therefore, to avoid this problem, the proposed system should be designed so that a Tx module is coupled with at least two Rx modules in an aligned case. Therefore, even if one of the modules is decoupled, the Tx side sees a load and non-zero coupling. Furthermore, Tx and Rx modules can be connected in series or parallel. In the proposed system, to increase the efficiency of the system, a parallel connection is used. Thus, the modules share the input and output current, and the ohmic losses decrease.

As a representative example of the proposed system, the 1Tx-2Rx system, as shown in Fig. 3, is analyzed in detail. If

the power ratings are desired to increase, the number of sets of 1Tx-2Rx can be increased. These sets can be connected in series to decrease the voltage stress of the semiconductors or in parallel to decrease the current stress.

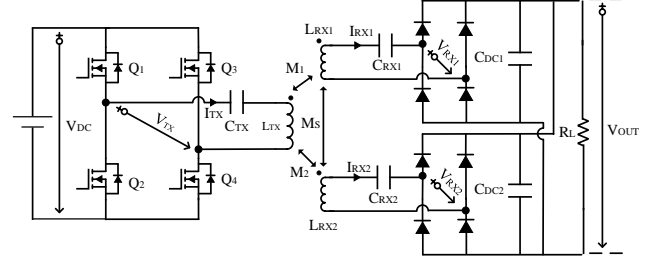


Fig. 2. The representation of 1Tx-2Rx series-series IPT system.

A. The System Parameters

The first harmonic approach of the 1Tx-2Rx system is given in Fig. 3.

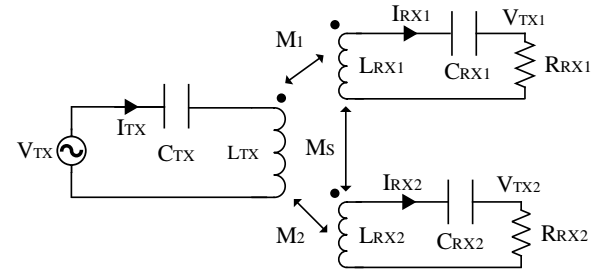


Fig. 3. First harmonic approach (FHA) model of the 1Tx-2Rx system.

The design parameters can be defined for a 1Tx-1Rx design, and later the Rx side can be divided into two parallel modules. The design methodology of 1Tx-1Rx series-series structures is well studied in the literature, and it is out of the topic of this paper. Therefore, the design steps in [23] are followed, and the parameters are found as given in Table I.

TABLE I
SYSTEM PROPERTIES AND KEY PARAMETERS

Number of Tx modules	1
Number of Rx modules	2
Power Rating	450 W
Input Voltage (V_{in})	60 V _{DC}
Output Voltage (V_{out})	36 V _{DC}
Resonant Frequency	160 kHz
Tx-Rx Magnetic Coupling	0.20
Rx module Cross-Coupling	-0.03
Rx side Quality Factor (Q_{Rx})	2.25
Tx Inductance (L_{Tx})	43.6 μ H
Tx Capacitance (C_{Tx})	22 nF
Rx Inductance (L_{Rx})	8.8 μ H
Rx Capacitance (C_{Rx})	109 nF
Load Resistance (R_L)	5 Ω

III. PROBLEM DEFINITION AND MATHEMATICAL MODEL

It is expected that parallel connected Rx modules share the current equally. However, it is observed that all current is drawn from the module that has a higher coupling coefficient, even if having a minor coupling difference. This is because the dominant module keeps the output voltage at its own voltage gain, and thus, the diodes of the recessive module are blocked. Fig. 4 shows the simulation results of receiver currents for the aligned and misaligned cases.

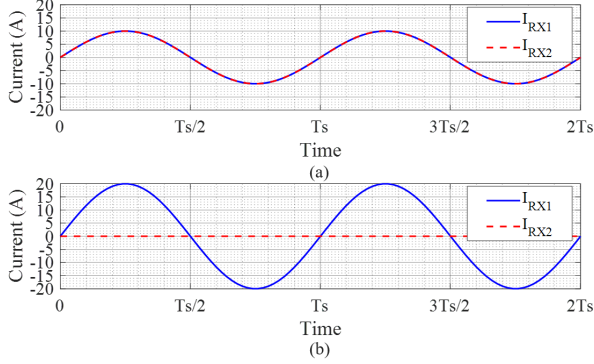


Fig. 4. Current waveforms of receivers in aligned and misaligned cases of the 1Tx-2Rx system.

For misaligned cases, coupling differences are kept at 10%, and it is observed that the current of the recessive module becomes zero. This unbalanced current sharing can be modeled by unequal reflected module resistance using the first harmonic approach (FHA). If there is single-Rx that is series compensated, the reflected resistance from the diode rectifier is calculated as in (1).

$$R_{RX} = \frac{8}{\pi^2} R_L \quad (1)$$

For the double-Rx system, the reflected resistances are doubled in the balanced case as in (2).

$$R_{RX(1)} = 2R_{RX}, R_{RX(2)} = 2R_{RX} \quad (2)$$

However, when the coupling coefficients between Tx and Rx's differ, the reflected resistances change drastically compared to the balanced case. Nevertheless, it should be considered that the total reflected resistance is the same as in (3).

$$\frac{1}{R_{RX}} = \frac{1}{R_{RX1}} + \frac{1}{R_{RX2}} \quad (3)$$

The induced voltages of Rx coils are calculated as in (4), which depends on the mutual inductance and Tx current. Besides, if the system operates at the resonant frequency, the output voltage of the receivers is equal to the induced voltage, and they should be equal in parallel connection as presented in (5).

$$\begin{aligned} V_{RX(1)_{induced}} &= j\omega M_{(1)} I_{TX} \\ V_{RX(2)_{induced}} &= j\omega M_{(2)} I_{TX} \end{aligned} \quad (4)$$

$$|V_{RX(1)}| = |V_{RX(2)}| = |V_{RX(1)_{induced}}| = |V_{RX(2)_{induced}}| \quad (5)$$

In Fig. 5, the lumped circuit of the receiver side is presented.

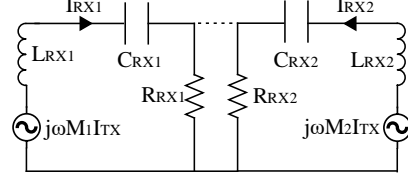


Fig. 5. The lumped circuit of parallel connected modules with receiver series compensation.

The module's voltages can be calculated as in (6) where $Z_{RX} = \frac{1}{j\omega C_{RX}} + j\omega L_{RX}$.

$$V_{RX(1)(2)} = R_{RX(1)(2)} \frac{j\omega M_{(1)(2)} I_{TX}}{Z_{RX} + R_{RX(1)(2)}} \quad (6)$$

Then, the equality condition of the module's voltages is obtained as in (7), and it is brought into a closed form, as given in (8) where α is defined as $\frac{M_1}{M_2}$.

$$|R_{RX(1)} \frac{M_1}{Z_{RX} + R_{RX(1)}}| = |R_{RX(2)} \frac{M_2}{Z_{RX} + R_{RX(2)}}| \quad (7)$$

$$0 = ((\alpha^2 - 1)R_L^2 - |Z_S|^2)R_1^2 + 2R_L R_1 + (\alpha^2 - 1)|Z_S R_L|^2 \quad (8)$$

The quadratic equation in (8) can be solved, and the reflected resistance of the first module can be calculated as in (9).

$$\begin{aligned} R_{RX(1)} &= \frac{R_{RX}|Z_{RX}|^2}{(1 - \alpha^2)R_{RX}^2 + |Z_{RX}|^2} \\ &+ R_{RX}Z_{RX} \frac{\sqrt{|Z_{RX}|^2\alpha^2 - R_{RX}^2(1 - \alpha^2)^2}}{(1 - \alpha^2)R_{RX}^2 + |Z_{RX}|^2} \end{aligned} \quad (9)$$

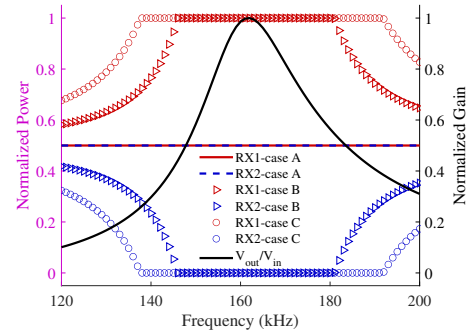


Fig. 6. The normalized power distribution of RX1 (the dominant module) and RX2 (the recessive module) for different cases (Case-A: Aligned, Case-B: 10% Misaligned, Case-C: 20% Misaligned.) and the normalized gain of the WPT system.

The normalized power distribution of $RX1$ (the dominant module) and $RX2$ (the recessive module) is plotted in Fig. 6 as a function of frequency for different cases of mutual differences. The power distribution at the resonant frequency is susceptible, and total power is undertaken by only one module, even if a slight change in mutual inductance. The power-sharing becomes better as the operation frequency is farther away from the resonant frequency. However, the gain of the WPT system is also decreasing while moving away from the resonant frequency, as given in Fig. 6. It means that the rated power cannot be achieved if the operation is moved away from the resonant frequency, even if the current sharing is balanced enough.

IV. CURRENT-SHARING PATH ANALYSES

The current sharing path can be used in order to avoid unbalanced current sharing at the operating frequency near the resonant frequency. The equivalent circuit of the 1Tx-2Rx system with the current sharing path is shown in Fig. 7.

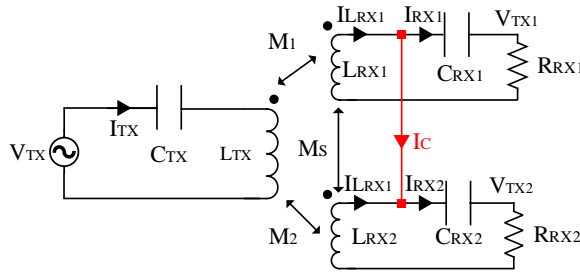


Fig. 7. FHA equivalent circuit of 1Tx-2Rx system with current sharing path.

With the current sharing path, the impedances which is seen by the receiver inductances (Z_{RX1} and Z_{RX2}) can be calculated as given in (10).

$$\begin{aligned} \frac{1}{Z_{RX1}} &= \frac{1}{\frac{1}{j\omega C_{RX1}} + R_{RX1}} + \frac{1}{\frac{1}{j\omega C_{RX2}} + R_{RX2}} \\ \frac{1}{Z_{RX2}} &= \frac{1}{\frac{1}{j\omega C_{RX1}} + R_{RX1}} + \frac{1}{\frac{1}{j\omega C_{RX2}} + R_{RX2}} \end{aligned} \quad (10)$$

Assuming the self-inductances and compensation capacitors are equal, it can be simplified as given in (11)

$$Z_{RX} = \frac{2}{j\omega C_{RX}} + R_{RX} \quad (11)$$

In this situation, it is observed that the reflected resistances to the receivers are independent of the mutual inductance, which guarantees that I_{RX1} is equal to I_{RX2} . However, coil currents differ from the receiver currents due to the circulation current, which can be calculated as in (12).

$$I_C = \frac{j\omega M_1 I_{TX} - j\omega M_2 I_{TX}}{L_{RX1} + L_{RX2}} \quad (12)$$

Due to the circulation current, the current sharing path may have some disadvantages in the cases of strong misalignment or faults. While a strong misalignment causes the quality factor of the system to change, short circuit or open circuit faults cause the system's efficiency to decrease.

A. Misalignment Analysis

Thanks to the current balancing path, the resistances of the receivers are equal for misaligned cases. Thus, it guarantees that the diode rectifiers share the current, which decreases the ohmic losses and gives better thermal management. However, with increasing misalignment between the receivers, the gain characteristic of the WPT system changes due to the variation of the reflected resistance to the Tx side, which can be calculated as given in (13).

$$\begin{aligned} Z_{TX} &= \frac{\omega^2 M_1^2}{L_{RX1} + \frac{Z_{RX1} L_{LRX2}}{Z_{RX1} + L_{RX2}}} + \frac{\omega^2 M_2^2}{L_{RX2} + \frac{Z_{RX2} L_{LRX1}}{Z_{RX2} + L_{RX1}}} \\ &= \frac{\omega^2 (M_1^2 + M_2^2)}{L_{RX} + \frac{Z_{RX} L_{LRX}}{Z_{RX} + L_{RX}}} \end{aligned} \quad (13)$$

The normalized gain for several misaligned cases is plotted in Fig. 8. In the misaligned cases, the operating frequency should be changed to achieve the desired gain, and in this situation, it is observed that the phase of Tx current (so power factor) changes, which increases the Tx current and decrease the efficiency as well.

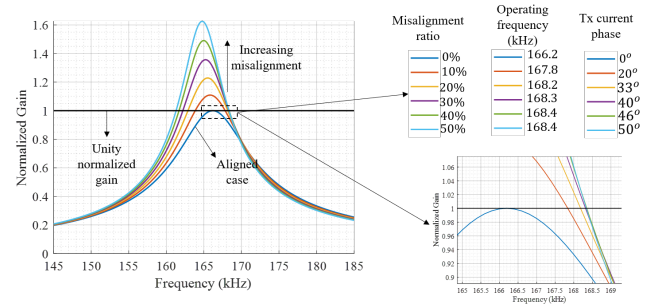


Fig. 8. The normalized gain of the WPT system for various misaligned cases and its operating frequencies and Tx current phases for these cases to achieve the unity normalized power.

Accordingly, for a specified misalignment, the current balancing path should be disconnected to increase the overall efficiency. The specified misalignment and the proposed switchable current balancing path will be discussed in Section V.

B. Fault Conditions

In healthy conditions within a specified misalignment, the current sharing path guarantees the balance current distribution of the receivers. However, the modular design should also provide a fault-tolerance, and the effect of the current sharing path on the fault conditions should be investigated. A common

fault in modular WPT is short-circuited coils. If one module becomes a short circuit, the other module behaves like a short circuit due to the current sharing path. Therefore, the system fault tolerance disappears. In order to avoid it, the induced voltages are tracked to monitor short-circuited coils, and the current-sharing path should be disconnected in this case. Accordingly, detecting the fault and disconnecting the current sharing path increases the system's reliability, and for this aim, a switchable current sharing path is required.

V. THE PROPOSED METHOD

Disadvantages of current sharing path proposed in [22] mainly caused by continuously connecting two receivers. In fault cases this connection causes high current flow through current sharing path which increases copper losses. Therefore, a new current balancing method, where the circuit diagram is given in Fig. 9, is implemented with self-controlled switches to turn off balancing in fault cases.

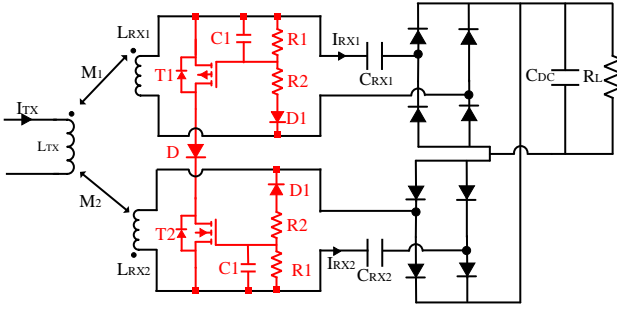


Fig. 9. The proposed 1Tx-2Rx IPT system with self-controlled current sharing path.

Proposed method has one switch for each receiver. These switches are ON if corresponding receiver coil's voltage is above a certain threshold. However, in shorted coil or in strong misalignment case, corresponding switch is turned off hence the current path is blocked.

Since induced voltages are AC, bidirectional switches are required for above mentioned operation. PMOS and NMOS switches have body diodes which prevents them to block current in both directions. There are several designs for bidirectional semiconductor switches [24] but most of them require additional components or gate drivers. To minimize the additional components, two semiconductor switches are used in such configuration that they can be controlled with receiver coil voltages without any gate drivers. MOSFET switches are placed in a way that their body diodes are in same direction. An opposing diode is placed in between these MOSFET's to block the body diodes. This configuration can block current in both direction and conduct in one direction. Therefore, balancing operation is done only in one half cycle. To allow bidirectional current flow, same switch set can be connected in antiparallel way. However, it is seen that balancing even in one half cycle boosts recessive side coil voltage and ensures balanced current sharing in both half cycles.

Gate voltages for the switches are generated from the receiver coils. However, gate voltage of a MOSFET must

be referenced to the source pin of the devices. Since both body diodes must be in same direction, one of the switches is selected as NMOS and the other one as PMOS. With this selection, generated gate voltages can be referenced to the source pin of corresponding switches. To ensure continuous conduction during balancing operation, receiver coil voltage is rectified through a diode and a capacitor to create constant gate signal for the switch. Since MOSFET gate current is nearly zero, generated gate voltage does not impact the receiver. Magnitude of the gate voltages are adjusted by the resistor voltage divider and limited with a zener protection diode. Selection of the resistors determine limit value of the misalignment which will be balanced.

A simulation setup is build to verify the operation of the design. Coupling of one receiver is changed during the simulation to observe the transient response. Limit for the misalignment is set to 50% with resistors as explained in the next section. As it can be seen in Fig. 10, switchable current sharing path is in conduction in 10% misaligned case and stops conducting at 55% misalignment. 10% misaligned receiver coil is shorted in the same simulation setup to observe the response in shorted coil fault. Results for this fault can be seen in Fig. 11

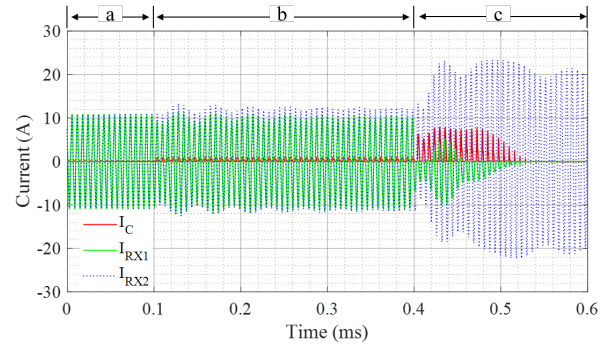


Fig. 10. Receiver coil currents and circulating current for (a) aligned, (b) 10% misaligned, (c) 55% misaligned case

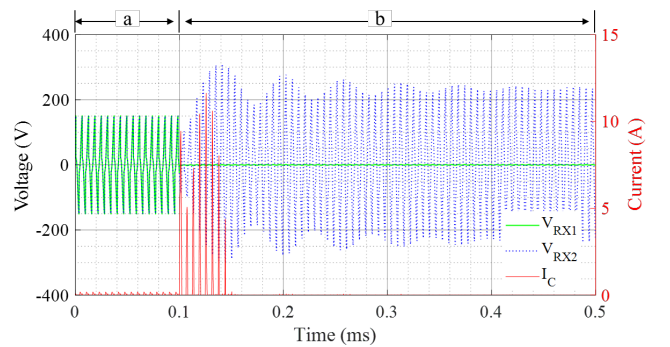


Fig. 11. Receiver coil voltages and circulating current before (a) and after (b) shorted receiver coil

A. Selection of the Resistors

Without balancing, current of the recessive side is almost zero. Therefore, it can be assumed that receiver coil voltage of

the recessive side has only induced voltage component from the transmitter side as in (4). However, transmitter current I_{Tx1} changes with misalignment due to change in transmitter side reflected resistance Z_{Tx} as given in (13). Assuming misalignment occurs in receiver 1, mutual inductance can be replaced with misalignment ratio (β) defined as $\frac{M_2 - M_1}{M_2}$. Neglecting transmitter coil resistance, transmitter current is directly proportional with $1/Z_{Tx}$ in resonance frequency. Therefore, using (13), ratio between the transmitter currents in aligned case and in misaligned case can be found as in (14).

$$\frac{T_{TX_{misaligned}}}{T_{TX_{aligned}}} = \frac{2M_2^2}{(M_1^2 + M_2^2)} = \frac{2M_2^2}{((1 - \beta)^2 M_2^2 + M_2^2)} = \frac{2}{(1 - \beta)^2 + 1} \quad (14)$$

Combining (4) and (14), induced voltage in receiver coil can be expressed in terms of aligned mutual inductance and aligned transmitter current as in (15)

$$V_{RX(i)} = j\omega(1 - \beta)M_2 I_{TX_{aligned}} \frac{2}{(1 - \beta)^2 + 1} \quad (15)$$

Gate voltage (V_{GS}) of the MOSFETS are equal to the corresponding capacitor voltages. At steady-state, DC current component of the capacitor is zero. Therefore, DC current component of R2 is equal to the DC current of R1. Current of R1 can be found as (16):

$$I_{R1_{DC}} = \frac{V_{C1}}{R1} \quad (16)$$

DC current component of R2 can be calculated with DC voltage component of R2. Since induced receiver coil voltage is sinusoidal and diode D1 blocks negative half-cycle, DC voltage of R2 can be found as (17):

$$V_{R2_{DC}} = \frac{\hat{V}_{RX(1)} - V_F - V_{C1}}{\pi} \quad (17)$$

$$I_{R2_{DC}} = \frac{V_{R2_{DC}}}{R2} = I_{R1_{DC}} = \frac{V_{C1}}{R1} \quad (18)$$

Combining (15), (17) and (18):

$$\begin{aligned} \frac{V_{C1}}{R1} &= \frac{\hat{V}_{RX(1)} - V_F - V_{C1}}{\pi R2} \\ &= \frac{\omega M_{(2)} I_{TX_{aligned}} \frac{2\sqrt{2}(1 - \beta)}{(1 - \beta)^2 + 1} - V_F - V_{C1}}{\pi R2} \end{aligned} \quad (19)$$

Where V_F is the forward voltage drop of D1. To find the resistor ratio for a given misalignment limit, $V_{C1} = V_{GS}$ in (19) can be set to $V_{GS(th)}$ to turn off the MOSFET at that point. Final form is then found as in (20)

$$\frac{R1}{R2} = \frac{\pi V_{GS(th)}}{(\omega M_{(2)} I_{TX} \frac{2\sqrt{2}(1 - \beta)}{(1 - \beta)^2 + 1}) - V_F - V_{GS(th)}} \quad (20)$$

VI. EXPERIMENTAL VALIDATION

An experimental setup of the 1Tx-2Rx system is established, shown in Fig. X. The system is tested in different cases. Firstly, the system is tested aligned and misaligned cases without the current sharing path. Then, the proposed switchable current sharing path is introduced, and the tests above are repeated. After that, the proposed and conventional systems are tested under strong misalignment and short-circuit fault cases. Finally, the efficiency measurements are taken for all these conditions to compare the proposed and conventional systems.

A. Tests of 1Tx-2Rx system without current balancing

The receiver currents are shown in Fig. X. for aligned and misaligned (20%) cases. As expected, for a small misalignment, the current of the recessive module is almost zero.

B. Tests of 1Tx-2Rx system with conventional and proposed current balancing methods

The receiver currents are shown in Fig. X. for aligned and misaligned (20%) cases with the conventional and proposed current sharing paths.

With the introduction of the current sharing path, the receiver current gets closer to each other. However, a circulation current exists, which increases with increasing misalignment.

Further, a voltage drop on the path due to MOSFETs and diode is observed in the proposed system, which decreases the efficiency compared to the conventional current-sharing path.

C. Tests of the 1Tx-2Rx system under strong misalignment and short circuit fault

The receiver currents are shown in Fig. X. for strong misalignment (50%) and short circuit fault with conventional and proposed current sharing paths.

In the conventional system, for strong misalignment, the circulating current is highly increasing, decreasing efficiency. Besides, in a short-circuit condition, the healthy module also behaves like short-circuit, and output power decreases as well.

The proposed method detects the strong misalignment and a short-circuits fault, and the current sharing path disconnects in these cases. Therefore, efficiency increases, and output power remains the same.

D. Efficiency Comparison

The efficiencies of the aligned and misaligned cases are compared in Table. X for the systems without a current sharing path, with the conventional current sharing path, and with the proposed current sharing path.

Further, the efficiencies of the conventional and proposed system are given in Table for strong misalignment and a short-circuit fault. X.

Although the proposed system efficiencies are slightly lower than the other systems for the aligned and misaligned case, the efficiencies become better in the case of strong misalignment and short-circuit fault.

VII. CONCLUSION

In this paper, a new switchable current sharing path for multi-receiver (multi-Rx) wireless power transfer (WPT) systems was presented. The current sharing path was analyzed mathematically, and it was observed that the circulation current is enormously increasing in cases of strong misalignment and fault. Therefore, a self-controlled switchable current-sharing path was introduced to disconnect the path in these cases. The proposed system was tested under different conditions with an experimental setup of a 1Tx-2Rx series-series compensated WPT system. It was observed that the efficiency of the system is increased by the proposed method in short-circuit fault and strong misalignment compared to the conventional system. Accordingly, with the proposed method, a modular system, which can be scaled according to the desired power level, can be achieved, which is both misalignment-tolerant and efficient.

REFERENCES

- [1] G. A. Covic and J. T. Boys, "Modern trends in inductive power transfer for transportation applications," *IEEE Journal of Emerging and Selected Topics in Power Electronics*, vol. 1, no. 1, pp. 28–41, 2013.
- [2] Q. Deng, Z. Li, J. Liu, S. Li, D. Czarkowski, M. K. Kazimierczuk, H. Zhou, and W. Hu, "Multi-inverter phase-shifted control for ipt with overlapped transmitters," *IEEE Transactions on Power Electronics*, vol. 36, no. 8, pp. 8799–8811, 2021.
- [3] Y. Zhang, S. Chen, X. Li, and Y. Tang, "Design methodology of free-positioning nonoverlapping wireless charging for consumer electronics based on antiparallel windings," *IEEE Transactions on Industrial Electronics*, vol. 69, no. 1, pp. 825–834, 2022.
- [4] X. Qu, H. Chu, S.-C. Wong, and C. K. Tse, "An ipt battery charger with near unity power factor and load-independent constant output combating design constraints of input voltage and transformer parameters," *IEEE Transactions on Power Electronics*, vol. 34, no. 8, pp. 7719–7727, 2019.
- [5] S. Y. R. Hui and W. W. C. Ho, "A new generation of universal contactless battery charging platform for portable consumer electronic equipment," *IEEE Trans. Power Electron.*, vol. 20, no. 3, pp. 620–627, 2005.
- [6] H. Hao, G. A. Covic, and J. T. Boys, "A parallel topology for inductive power transfer power supplies," *IEEE Trans. Power Electron.*, vol. 29, no. 3, pp. 1140–1151, 2014.
- [7] Z. Wang, X. Cao, Y. Zhu, Y. Zhu, Q. Cai, and J. Fan, "Five-coil wireless charging structure with radiated slots in uavs for mutual inductance reduction," in *2021 International Applied Computational Electromagnetics Society (ACES-China) Symposium*, 2021, pp. 1–2.
- [8] S. Moon and G.-W. Moon, "Wireless power transfer system with an asymmetric four-coil resonator for electric vehicle battery chargers," *IEEE Transactions on Power Electronics*, vol. 31, no. 10, pp. 6844–6854, 2016.
- [9] H. Chen, Z. Qian, R. Zhang, Z. Zhang, J. Wu, H. Ma, and X. He, "Modular four-channel 50 kw wpt system with decoupled coil design for fast ev charging," *IEEE Access*, vol. 9, pp. 136 083–136 093, 2021.
- [10] H. Zhou, J. Chen, Q. Deng, F. Chen, A. Zhu, W. Hu, and X. Gao, "Input-series output-equivalent-parallel multi-inverter system for high-voltage and high-power wireless power transfer," *IEEE Transactions on Power Electronics*, vol. 36, no. 1, pp. 228–238, 2021.
- [11] G. Ning, K. Zhao, and M. Fu, "A passive current sharing method for multitransmitter inductive power transfer systems," *IEEE Transactions on Industrial Electronics*, vol. 69, no. 5, pp. 4617–4626, 2022.
- [12] H. Hu, S. Duan, T. Cai, and P. Zheng, "A current-sharing compensation method for high-power-medium-frequency coils composed of multiple branches connected in parallel," *IEEE Transactions on Industrial Electronics*, vol. 69, no. 5, pp. 4637–4651, 2022.
- [13] G. Ke, Q. Chen, W. Gao, S.-C. Wong, C. K. Tse, and Z. Zhang, "Research on ipt resonant converters with high misalignment tolerance using multicoil receiver set," *IEEE Transactions on Power Electronics*, vol. 35, no. 4, pp. 3697–3712, 2020.
- [14] H. He, Y. Liu, B. Wei, C. Jiang, S. Wang, X. Wu, and B. Jiang, "Circulating current suppression and current sharing strategy for parallel ipt system based on d-q synchronous rotating frame," *CSEE Journal of Power and Energy Systems*, pp. 1–14, 2022.
- [15] M. Bojarski, E. Asa, K. Colak, and D. Czarkowski, "Analysis and control of multiphase inductively coupled resonant converter for wireless electric vehicle charger applications," *IEEE Transactions on Transportation Electrification*, vol. 3, no. 2, pp. 312–320, 2017.
- [16] Q. Deng, J. Liu, D. Czarkowski, W. Hu, and H. Zhou, "An inductive power transfer system supplied by a multiphase parallel inverter," *IEEE Transactions on Industrial Electronics*, vol. 64, no. 9, pp. 7039–7048, 2017.
- [17] G. Ning, S. Wang, G. Zheng, Y. Liu, and M. Fu, "A novel passive current sharing method for a two-transmitter one-receiver wpt system," in *2020 IEEE 9th International Power Electronics and Motion Control Conference (IPEMC2020-ECCE Asia)*, 2020, pp. 985–990.
- [18] G. Ning, K. Zhao, and M. Fu, "A passive current sharing method for multitransmitter inductive power transfer systems," *IEEE Transactions on Industrial Electronics*, vol. 69, no. 5, pp. 4617–4626, 2022.
- [19] H. Wang, Y. Chen, and Y.-F. Liu, "A passive-impedance-matching technology to achieve automatic current sharing for a multiphase resonant converter," *IEEE Transactions on Power Electronics*, vol. 32, no. 12, pp. 9191–9209, 2017.
- [20] H. Polat, E. Ayaz, O. Altun, and O. Keysan, "Balancing of common dc-bus parallel-connected modular inductive power transfer systems," *IEEE Journal of Emerging and Selected Topics in Power Electronics*, vol. 10, no. 2, pp. 1587–1596, 2022.
- [21] E. Ayaz, O. Altun, H. Polat, and O. Keysan, "Fault tolerant multi-tx/multi-rx inductive power transfer system with a resonator coil," *IEEE Journal of Emerging and Selected Topics in Power Electronics*, vol. 11, no. 1, pp. 1272–1284, 2023.
- [22] G. Ning, P. Zhao, R. He, and M. Fu, "A novel passive current sharing method for a two-receiver-coil ipt system," in *2020 IEEE PELS Workshop on Emerging Technologies: Wireless Power Transfer (WoW)*, 2020, pp. 354–357.
- [23] O. Altun, E. Ayaz, H. Polat, and O. Keysan, "A modular inductive power transfer system for synchronous machine field excitation," in *2022 Wireless Power Week (WPW)*, 2022, pp. 476–481.
- [24] H. Dai, R. A. Torres, T. M. Jahns, and B. Sarlioglu, "Characterization and implementation of hybrid reverse-voltage-blocking and bidirectional switches using wbg devices in emerging motor drive applications," in *2019 IEEE Applied Power Electronics Conference and Exposition (APEC)*, 2019, pp. 297–304.